2-1-2008

Interactions between bacterial carbon monoxide and hydrogen consumption and plant development on recent volcanic deposits

Gary M. King
Louisiana State University

Carolyn F. Weber
Louisiana State University

Recommended Citation

King, G., & Weber, C. (2008). Interactions between bacterial carbon monoxide and hydrogen consumption and plant development on recent volcanic deposits. *ISME Journal, 2* (2), 195-203. https://doi.org/10.1038/ismej.2007.101

The ISME Journal (2008) 2, 195–203

www.nature.com/ismej

ORIGINAL ARTICLE

Interactions between bacterial carbon monoxide and hydrogen consumption and plant development on recent volcanic deposits

Gary M King and Carolyn F Weber
Department of Biological Sciences, Louisiana State University, Baton Rouge, LA, USA

Patterns of microbial colonization and interactions between microbial processes and vascular plants on volcanic deposits have received little attention. Previous reports have shown that atmospheric CO and hydrogen contribute significantly to microbial metabolism on Kilauea volcano (Hawaii) deposits with varied ages and successional development. Relationships between CO oxidation and plant communities were not clear, however, since deposit age and vegetation status covaried. To determine plant–microbe interactions in deposits of uniform ages, CO and hydrogen dynamics have been assayed for unvegetated tephra on a 1959 deposit at Pu'u Puai (PP-bare), at the edge of tree 'islands' within the PP deposit (PP-edge) and within PP tree islands (PP-canopy). Similar assays have been conducted for vegetated and unvegetated sites on a 1969 Mauna Ulu (MU) lava flow. Net *in situ* atmospheric CO uptake was highest at PP-edge and PP-bare sites (2.2 ± 0.5 and 1.3 ± 0.1 mg CO m^{-2} day^{-1}, respectively), and least for PP-canopy (-3.2 ± 0.9 mg CO m^{-2} day^{-1}, net emission). Respiration rates, microbial biomass and maximum CO uptake potential showed an opposing pattern. Comparisons of atmospheric CO uptake and CO_2 production rates indicate that CO contributes significantly to microbial metabolism in PP-bare and MU-unvegetated sites, but negligibly where vegetation is well developed. Nonetheless, maximum potential CO uptake rates indicate that CO oxidizer populations increase with increasing plant biomass and consume CO actively. Some of these CO oxidizers may contribute to elevated nitrogen fixation rates (acetylene reduction) measured within tree islands, and thus, support plant successional development.
The ISME Journal (2008) **2,** 195–203; doi:10.1038/ismej.2007.101; published online 29 November 2007
Subject Category: microbial ecology and functional diversity of natural habitats
Keywords: biogeochemistry; carbon monoxide; volcanic

Introduction

Volcanic landscapes typically consist of a mosaic of successional states (Kitayama *et al.*, 1995). Deposit age, degree of weathering, precipitation, temperature and availability of potential colonists interact with other variables to determine patterns of ecosystem development at local-to-regional scales (Chadwick *et al.*, 1999; Morisada *et al.*, 2002). Analyses of these patterns have contributed to the formulation of ecological theories and to a greater understanding of biogeochemical controls of ecosystem dynamics (Hooper and Vitousek, 1997; Vitousek and Farrington, 1997; Chadwick *et al.*, 1999). For instance, the roles of phosphorus, nitrogen and eolian nutrient inputs have been clearly documented through long-term observations of Hawaiian chronosequences (Crews *et al.*, 1995; Chadwick *et al.*, 1999; Neff *et al.*, 2000).

Although they are among the first arrivals on volcanic deposits, relatively little is known about the temporal and spatial distributions of microbial colonists generally, about specific microbial functional groups or about interactions among microorganisms and animal and plant communities. Vitousek and co-workers have addressed some of these issues through their research on nitrogen fixation and nitrogen mineralization on Hawaiian volcanic deposits (Riley and Vitousek, 1995; Vitousek, 1999; Crews *et al.*, 2001; Pearson and Vitousek, 2001). Nüsslein and Tiedje (1998), Nanba *et al.* (2004) and Dunfield and King (2004) have documented various aspects of microbial community structure and function on recent Hawaiian volcanic deposits (44–300 years old), and shown in particular

Correspondence: GM King, Department of Biological Sciences, Louisiana State University, 202 Life Sciences Building, Baton Rouge, LA 70808, USA.
E-mail: gking@lsu.edu
Received 28 June 2007; revised 2 October 2007; accepted 2 October 2007; published online 29 November 2007

that relatively young deposits harbored very distinct assemblages, especially where plants were present. Analyses of quinone profiles on Mt Pinatubo mudflows also suggested possible associations of *Actinobacteria* with developing plant communities (Ohta *et al.*, 2003).

Other groups have reported variable relationships among plant community development, heterotrophic evenness, respiration, and C, N and P contents for successional transects on volcanic soils (Schippers *et al.*, 2001). A survey of older soils of Mt Etna has also shown that respiration varied independently of soil carbon content, and that plant litter decomposition varied as a function of soil development and plant litter source (Hopkins *et al.*, 2007).

King (2003a) showed that microbial uptake of atmospheric CO and hydrogen accounted for a significant fraction of respiratory metabolism on volcanic deposits ranging from about 21–210 years in age, but that these processes were relatively unimportant at a 300-year-old site supporting a mature forest. Results from Dunfield and King (2004, 2005) and Gomez-Alvarez *et al.* (2007) also showed that microbial community structure changed markedly along this chronosequence, with both CO oxidizers and the microbial community as a whole dominated by *Proteobacteria* in the forested site, while other phyla, including many unidentified lineages, dominated the remaining sites.

The observed patterns along the chronosequence may partially reflect factors such as physical weathering, accumulated inputs of microbes from the atmosphere, and various stochastic and deterministic processes independent of plant succession. They also undoubtedly reflect plant-dependent interactions. These may include species-specific interactions, such as those between actinorhizal or legume species (Ohtonen and Väre, 1998; Smolander and Kitunen, 2002; de Neergaard and Gorissen, 2004) and their symbionts, or more general interactions, such as those resulting from inputs of organic matter (Kent and Triplett, 2002). Similar conclusions have been drawn for successional patterns associated with glacial retreat (Ohtonen *et al.*, 1999; Sigler *et al.*, 2002; Sigler and Zeyer, 2002).

Results presented here document interactions between plant succession and CO dynamics on volcanic deposits independent of substrate age. CO uptake rates at atmospheric and elevated concentrations and comparisons of activities across gradients of plant development on volcanic deposits of a single age show that atmospheric CO is consumed most rapidly in deposits with little or no rooted vegetation. In contrast, maximum potential uptake rates, an index of CO oxidizer biomass, are greatest where plant development and organic matter are greatest. These results suggest that after initial colonization of newly formed substrates, CO oxidizer populations likely depend on organic inputs from plant communities for significant growth. Some of these CO oxidizers may contribute to increases in acetylene reduction rates (King, 2003a), an index of nitrogen fixation, that were observed with increasing root biomass.

Materials and methods

Site description

Sites were established near Kilauea caldera on a 1959 tephra deposit (Pu'u Puai—PP) and a 1969 lava flow (Mauna Ulu—MU), aspects of which have been previously described (King, 2003a; Dunfield and King, 2004; Nanba *et al.*, 2004; Gomez-Alvarez *et al.*, 2007). The PP site consists of islands of closed-canopy woody vegetation (mixed *Metrosideros polymorpha* (Ohia) and *Morella faya* (also *Myrica faya* or fire tree) interspersed with extensive unvegetated patches comprised of tephra (or volcanic cinders); the cinders were approximately 1 cm in diameter. At PP, samples were collected within tree islands (PP-canopy), at the island edges 3–5 m from canopy centers (PP-edge) and 5 m distant from islands in unvegetated tephra (PP-bare). A pronounced litter layer (approximately 5–10 cm thick) occurred within and at the edge of tree islands, while at bare sites, little or no litter was present. At MU, samples were collected from cinder deposits that had accumulated on the surface of pahoehoe lava. Vegetation at MU is more patchy and sparse than at PP. Sample sites were colonized by a pioneering fern, *Sadleria cyatheoides* (MU-veg) or were unvegetated (MU-unveg).

Bulk physical and chemical analyses

Aluminum core tubes (7.2-cm inner diameter) were used to collect material to 5–10 cm depths. Water contents were estimated by drying at 110 °C for >24 h. pH was determined using slurries of cinders and deionized water (1:2 mass ratio of samples and deionized water). Total organic carbon and nitrogen were analyzed using a Perkin–Elmer model 2400 elemental analyzer for ground material from the upper two centimeters. Root biomass was determined by harvesting fine roots (<2-mm diameter) from the upper 10 cm of material at each site.

Phospholipid phosphate analysis

Phospholipid phosphate contents were analyzed as a surrogate for microbial biomass (Brinch-Iversen and King, 1990). Triplicate 0.5- to 1-gram fresh weight (gfw) root-free samples from various depths were transferred to screw-cap glass tubes containing 5 ml of a 1:2 mixture of dichloromethane /methanol. The tubes were sealed, transported to the laboratory on dry ice and subsequently stored at -20 °C prior to further processing. Dichloromethane (1.67 ml) and deionized water (5 ml) were added to each tube prior to centrifugation (1000 *g*). Dichloromethane (1–2 ml) phases were transferred to glass ampoules and

evaporated to dryness at 30 °C with nitrogen. Phospholipid phosphate was liberated by persulfate digestion and measured colorimetrically (Brinch-Iversen and King, 1990).

Gas flux analyses

Carbon monoxide and hydrogen fluxes were measured *in situ* using aluminum collars (about 67 cm^2) fitted with a 1-l quartz chamber forming a static headspace (see King, 2003a). Gas exchange assays were initiated by sealing a chamber to a collar, covering the chamber with aluminum foil, and removing 3-cm^3 headspace samples using a needle and syringe at 3- to 4-min intervals for up to 15–20 min. Samples were assayed in the field using a Trace Analytical RGD gas chromatograph (King, 1999). Starting ambient CO and hydrogen values were typically about 100 and 550 p.p.b., respectively.

Additional assays were conducted using triplicate intact cores (7.5-cm inner diameter × 20-cm length). Triplicate cores from PP and MU sites were returned to a field laboratory within a few hours after collection and incubated at ambient temperature. After sealing the core tubes, core headspaces were subsampled for CO and hydrogen analysis as above. Analyses of CO_2 production were performed using headspace samples that were injected into an SRI flame ionization gas chromatograph equipped with a stainless steel column (3.2-mm outer diameter × 2 m) containing silica gel and a methanizer to convert CO_2 into methane. Samples for CO_2 production were collected at intervals over a 48-h period during incubations at ambient temperature. Instrument responses to CO_2 and methane were determined using standards prepared from pure gases. Responses to CO and hydrogen were determined using standards at near-atmospheric levels or greater; they were prepared by diluting pure gases in CO- and hydrogen-free air.

Maximum potential CO and hydrogen uptake rates were estimated using fresh material from the upper 2-cm depth interval of each PP and MU site. Triplicate 5-gfw samples were transferred to 110-cm^3 jars that were sealed with neoprene stoppers and incubated in darkness at ambient temperature. After adding CO or hydrogen to a final concentration of about 100 parts per million (p.p.m.; 1 p.p.m. is equivalent to about 0.1 kPa), jar headspaces were subsampled at intervals to determine uptake rates. Maximum potential CO uptake rates were also estimated for selected depth intervals of PP sites. Similar assays were conducted with freshly collected, washed, soil-free fine (< 2 mm) roots from *M. polymorpha*, *M. faya* and *S. cyatheoides*; triplicate samples of approximately 1 gfw of each root type were incubated in darkness in sealed jars with an ambient atmosphere (0.1 p.p.m. CO) and with 100 p.p.m. CO as described by King and Crosby (2002).

Acetylene reduction rates

Triplicate intact cores (about 10 cm deep) from each of the PP and MU sites were collected using aluminum core tubes (7.2-cm inner diameter). Acetylene was added to the core headspaces to a final concentration of about 5%. Sealed tubes were incubated at ambient temperature for about 72 h. Headspace samples were obtained at intervals and transferred to evacuated 3-cm^3 gas collection tubes containing 0.5 ml of ammoniacal silver nitrate to precipitate acetylene. Ethylene (C_2H_4) concentrations in subsamples were analyzed by flame ionization gas chromatography using a Shimadzu GC-14A. Rates of C_2H_4 production provided a surrogate estimate of N_2-fixation rates.

Results

Bulk deposit properties

Root biomass varied dramatically among sites (Table 1) with a maximum in vegetated areas of 652 ± 165 gram dry weight (gdw) per m^2 for PP-canopy and minimum of 50 ± 4 gdw m^{-2} for MU-veg. Unvegetated PP and MU sites contained negligible identifiable root mass. Total carbon and nitrogen contents paralleled root distributions with values up to 45.7 and 1.7%, respectively, in PP-canopy. C/N ratios were least in PP-bare (15.7), increasing by

Table 1 Selected properties of Pu'u Puai and Mauna Ulu volcanic deposits

Variable	*Pu'u Puai*			*Mauna Ulu*	
	Canopy	*Edge*	*Bare*	*Vegetated*	*Unvegetated*
Root mass	652 (165)	151 (35)	< 5	50 (4)	< 5
Phospholipid phosphate	139 (11)	10 (1)	14.3 (1)	7 (1)	1 (0.2)
% carbon	45.7 (0.8)	2.8 (0.5)	0.33 (0.10)	15.3 (2.1)	0.21 (0.02)
% nitrogen	1.7 (0.02)	0.12 (0.02)	0.02 (0.01)	0.61 (0.04)	ND
C/N ratio	27.2	23.1	15.7	25.2	—
pH	3.9 (0.2)	4.5 (0.2)	6.9 (0.1)	5.8 (0.2)	6.5 (0.3)
Water content	241	14.6	1.2	1.8	0.8

Root mass, (0–10 cm), gram dry weight (gdw) per m^2; phospholipid phosphate (nmol P gdw^{-1}), % C, % N, pH and water content (mg water per gdw) from 0- to 2-cm depth interval. Water contents from duplicate determinations; all other data are means of triplicates (± 1 s.e.).

almost twofold in PP-canopy (27.2). In contrast, pH values decreased substantially from 6.9 in PP-bare to 3.9 in PP-canopy. Water contents displayed the opposite trend, with PP-bare material holding very little water, while PP-edge and PP-canopy were relatively moist by comparison. Trends between MU-unveg and MU-veg were comparable (Table 1).

Phospholipid phosphate content

Phospholipid phosphate concentrations varied substantially among sites and with deposit depth (Figure 1). PP-canopy surface material contained phospholipid concentrations more than an order of magnitude higher than surface material from any other site ($P<0.001$, analysis of variance). Phospholipid phosphate concentrations were similar, however, for PP-edge and PP-bare sites at all depths. At all PP sites, phospholipid phosphate concentrations decreased by an order of magnitude with increasing depth up to 10 cm; these changes were statistically significant ($P<0.01$, analysis of variance). At MU-veg, phospholipid phosphate concentrations were an order of magnitude greater than at MU-unveg ($P<0.01$), and about 20-fold lower than at corresponding PP sites.

Gas exchange

Volcanic deposits at three of five sites consistently consumed atmospheric CO: PP-bare, MU-veg and MU-unveg (Table 2). CO was emitted consistently from PP-canopy, but results were more variable for PP-edge, with both uptake and emission observed (Table 2). Atmospheric CO uptake rates ranged between about 1.2 and 8.1 mg $CO\,m^{-2}\,day^{-1}$, with no clear trends among sites. CO emission rates ranged from about 1.3 to 8.1 mg $CO\,m^{-2}\,day^{-1}$ (Table 2) for PP-canopy, with intermediate PP-edge values. *In situ* CO exchange rates were similar to those for values obtained from *ex situ* incubation of intact cores (Table 2). Estimates for steady-state CO exchange concentrations (concentrations at which CO uptake equals CO production) ranged between 0 and 21 p.p.b. (parts per billion) for all but the PP-canopy site (Table 2). For the latter, the steady-state concentration was 207 ± 43 p.p.b., well above the typical ambient atmospheric concentrations (75–125 p.p.b.). CO uptake rate constants were lowest in PP-canopy and MU-unveg ($0.1\,min^{-1}$) and significantly higher for the remaining sites (Table 2).

For the MU sites, maximum potential CO uptake rates (0- to 2-cm depth interval) were significantly greater ($P<0.01$) at MU-veg than MU-unveg. The MU values, however, were substantially less than values for comparable PP sites (Table 2). At PP-canopy and PP-edge sites, maximum potential CO uptake rates decreased significantly (analysis of variance, $P<0.01$) with deposit depth (Figure 1a). For the 0- to 2-cm and 2- to 5-cm depth intervals, PP-canopy and PP-edge rates were similar, but PP-canopy rates were significantly greater for the 5- to 10-cm interval. In contrast, maximum potential CO uptake rates were least for PP-bare, and did not decline significantly with depth. With the exception of a single apparent outlier for the 0- to 2-cm depth interval of PP-edge, maximum potential CO uptake rates were strongly correlated ($r=0.99$) with phospholipid phosphate concentrations (Figure 1b); a strong correlation ($r=0.74$) remains even if the apparent outlying point is included.

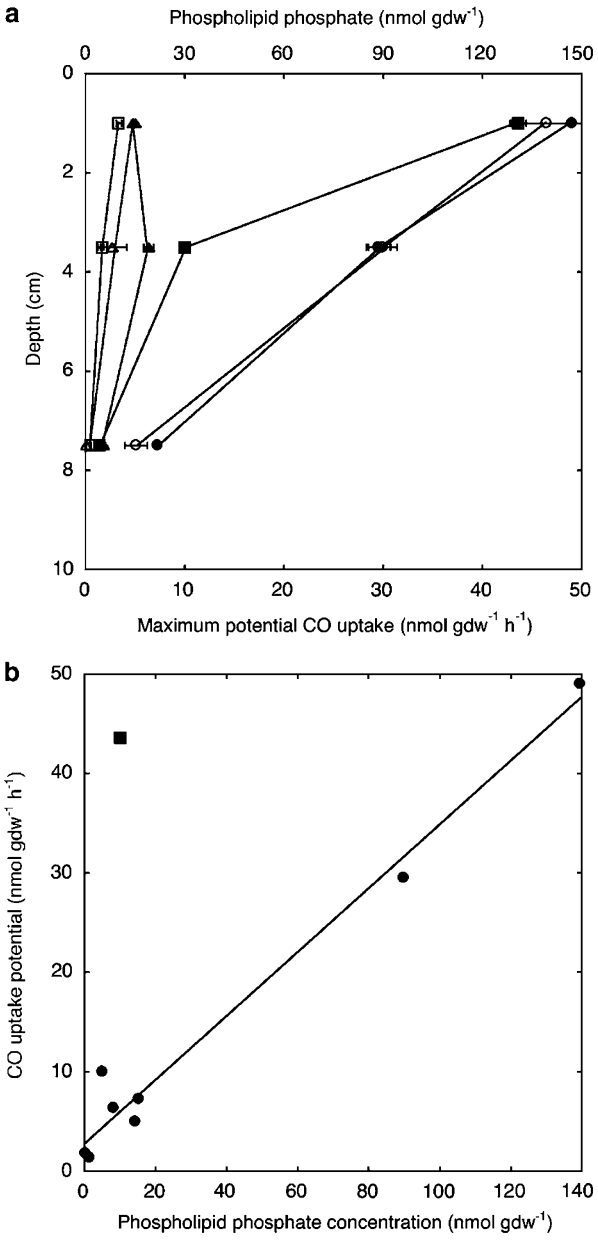

Figure 1 (**a**) Depth profiles of phospholipid phosphate concentration (closed symbols) and maximum potential CO uptake rates (open symbols) for Pu'u Puai (PP)-bare (triangles), -edge (squares), and -canopy (circles) sites. All data are means of triplicate determinations ±1 s.e. (**b**) Correlation between maximum potential CO uptake rates and phospholipid phosphate concentrations for all sites, excluding the 0- to 2-cm interval of PP-edge (square).

Table 2 Gas exchange rates for Pu'u Puai and Mauna Ulu sites

Variable	*Pu'u Puai*			*Mauna Ulu*	
	Canopy	*Edge*	*Bare*	*Vegetated*	*Unvegetated*
Ex situ, net exchange	−1.3 to −8.1	−3.9 to 3.2	1.7–8.1	3.0–4.2	1.2–3.9
Steady-state CO	207 (43)	21 (7)	7 (1)	9 (1)	0
Uptake rate constant	0.1 (0.03)	1.0 (0.2)	0.3 (0.02)	0.4 (0.04)	0.1 (0.01)
Respiration rate, mol	103.7 (22.8)	50.8 (6.4)	3.2 (0.6)	74.2 (26.5)	2.2 (0.5)
Respiration rate, mass	4.56 (1.0)	2.24 (0.28)	0.14 (0.03)	3.26 (1.16)	0.10 (0.02)
% CO of respiration	0	0	9.1	0.2	6.4
In situ, net exchange	−3.2 (0.9)	2.2 (0.5)	1.3 (0.1)	—	—
Maximum CO uptake	92.5 (6.3)	88.2 (5.4)	26.0 (3.6)	53.2 (2.3)	19.2 (5.4)
Ex situ hydrogen uptake	1.4 (0.3)	2.9 (1.5)	2.4 (0.3)	2.9 (0.6)	2.1 (0.4)
Acetylene reduction rate	21.5 (11.9)	1.6 (1.0)	0.8 (0.8)	2.2 (0.7)	0.4 (0.4)

Ex situ and *in situ* CO and hydrogen exchanges under ambient conditions in mg CO or H_2 per m^2 per day (negative values indicate CO emission); steady-state CO concentration, parts per billion (p.p.b.); uptake rate constant, min^{-1}; respiration rates are given in mmol CO_2 per m^2 per day (mol) and $g\,m^{-2}\,day^{-1}$ (mass); acetylene reduction rate in nmol acetylene reduced per m^2 per day; maximum CO uptake rate units are given in nmol $gdw^{-1}\,d^{-1}$. All data are means of triplicates (±1 s.e.).

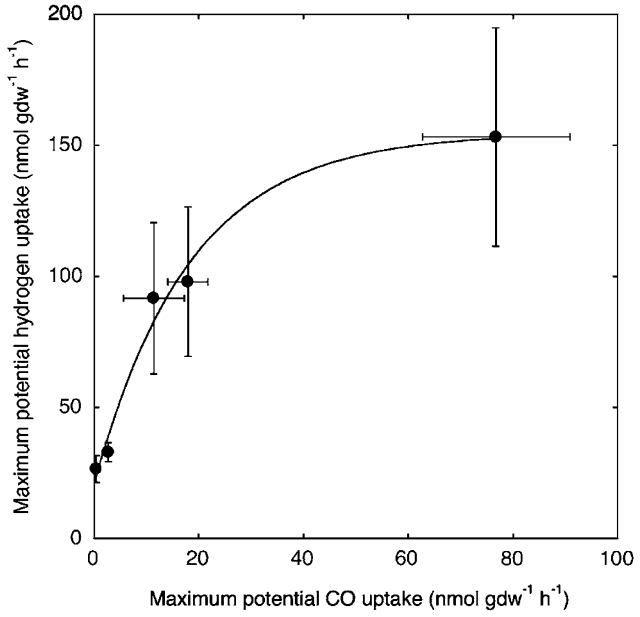

Figure 2 Maximum potential hydrogen uptake versus maximum potential CO uptake rates for the 0- to 2-cm depth interval of all sites. All data are means of triplicates ±1 s.e. Curve represents a nonlinear best fit to an exponential rise to an asymptote ($r^2 = 0.98$).

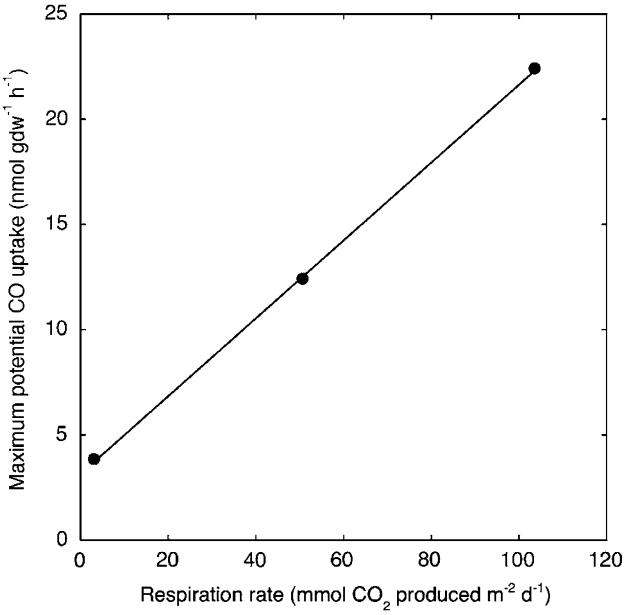

Figure 3 Correlation between maximum potential CO uptake rates and root biomass. All data are means of triplicates ±1 s.e. Curve represents a linear fit ($r = 0.99$).

All sites consumed atmospheric hydrogen at rates generally greater than those for CO (Table 2). Trends in uptake versus vegetational development among sites were not statistically significant ($P > 0.5$, analysis of variance), although activity at PP-canopy was least with the highest threshold value (Table 2). Hydrogen was also consumed during *ex situ* assays to determine maximum potential uptake rates. Maximum potential hydrogen uptake rates were greater than the corresponding maximum potential CO uptake rates at all sites, and increased from MU-unveg to PP-canopy. A plot of paired maximum potential hydrogen uptake and maximum potential CO uptake rates indicated that the capacity for hydrogen uptake rose exponentially to an asymptotic maximum as a function of increased CO uptake capacity (Figure 2).

Respiration rates, measured as CO_2 production, increased with increasing vegetational development, and ranged from 3.2 ± 0.6 to 103.7 ± 22.8 and from 2.2 ± 0.5 to $74.2 \pm 26.5\,mmol\,m^{-2}\,day^{-1}$ for PP and MU sites, respectively (Table 2). Maximum potential CO uptake rates for the 0- to 2-cm interval of all sites were positively and linearly correlated with respiration rates ($r = 0.71$); maximum CO uptake potentials integrated over 0- to 10-cm depth for the PP sites were highly linearly correlated with respiration rates ($r = 0.99$; Figure 3). The relative contribution of atmospheric CO uptake to respiratory reducing equivalent flow for PP and MU was

estimated by assuming a 1:1 stoichiometry for CO_2 production and oxygen uptake, and two and four reducing equivalents formed per mole of CO oxidized and CO_2 produced, respectively. The percent of total respiratory reducing equivalent flow due to CO was calculated as:

$$\text{mol CO oxidized}/[2\times(\text{mol CO}_2\text{ produced} - \text{mol CO oxidized})]. \quad (1)$$

Since both PP-canopy and PP-edge sites emitted CO during the time the respiration assay was conducted, the relative contribution of CO to respiratory reducing equivalent flow was zero; for PP-bare, a value of 9.1% was obtained. For MU sites, the values ranged from negligible at MU-veg (0.2%) to 6.4% at MU-unveg (Table 2).

Acetylene reduction

Acetylene reduction rates were least in MU-unveg and PP-bare sites (0.4–0.8 μmol C_2H_2 reduced per m^2 per day) and reached a maximum for PP-canopy samples (21.5 μmol C_2H_2 reduced per m^2 per day; Table 2). Acetylene reduction rates were positively and linearly correlated with root biomass across all sites ($r=0.98$), and positively and exponentially correlated with respiration rates ($r=0.95$). In addition, acetylene reduction rates increased exponentially with increasing maximum CO uptake potential rates integrated over 10 cm depth for the PP sites ($r=0.99$); comparable depth profiles were not available for the MU sites.

Root CO production and oxidation

Live, fine roots from the fern, *S. cyatheoides*, and the trees, *M. polymorpha* and *M. faya*, each produced CO when incubated under ambient conditions. CO production rates for *S. cyatheoides* roots obtained from two distinct sites (MU and a 1982 lava flow; 1.9–3.3 nmol $gfw^{-1}\,h^{-1}$, respectively) were comparable to rates for *M. faya*, 3.5 ± 0.3 nmol $gfw^{-1}\,h^{-1}$ and *M. polymorpha*, 1.2 ± 0.1 nmol $gfw^{-1}\,h^{-1}$ (Table 3). Maximum potential CO uptake rates were considerably higher than CO production rates, and varied significantly among the three taxa. Essentially, identical uptake rates were observed for the two sets of *S. cyatheoides* roots, 12.8 ± 1.6 nmol CO oxidized per gfw per h. Uptake rates for *M. polymorpha* (9.6 ± 0.6 nmol CO oxidized per gfw per h) were somewhat lower, while rates for *M. faya* (24.4 ± 1.6 nmol CO oxidized per gfw per h) were somewhat higher. In general, there was a positive correlation between maximum potential root CO oxidation rates and root CO production rates ($r=0.9$; not shown).

Table 3 CO production under ambient conditions and CO uptake during incubation with 100 p.p.m. CO by washed, soil-free fine roots of *Sadleria cyatheoides*, *Metrosideros polymorpha* and *Morella faya*

Plant	*CO production*	*CO oxidation*
S. cyatheoides	1.9 ± 3.3	12.8 ± 0.6
M. polymorpha	1.2 ± 0.1	24.4 ± 1.6
M. faya	3.5 ± 0.3	9.6 ± 0.6

All data are nmol per gfw per h and means of triplicates (± 1 s.e.).

Discussion

Analyses of receding glaciers and chronosequences of volcanic systems have revealed several aspects of microbial community responses to ecosystem succession, including temporal and spatial changes in functional diversity, phylogenetic diversity (evenness and richness) and cell-specific activities. For example, Sigler *et al.* (2002) observed increases in cell number and total activity with successional age, but maximal activity per cell and greater relative culturability occurred at intermediate stages, and phylotype richness decreased with age. Their results confirmed an 'r-' to 'K-strategy' shift during succession, but indicated that successional changes were dynamic and occurring at both individual and community levels. Others have documented interactions between microbes and vegetation, including changes in carbon utilization and community structure (for example, Ohtonen *et al.*, 1999; Schipper *et al.*, 2001).

Previous analyses of Kilauea volcano based on multiple sites that constituted a chronosequence from 21- to 300-year old showed that atmospheric CO and hydrogen utilization occurred early in successional development and contributed significantly to respiratory metabolism (King, 2003a). Molecular ecological analyses also revealed significant differentiation among CO-oxidizing and lithotrophic communities colonizing deposits of different ages and successional development (Dunfield and King, 2004, 2005; Nanba *et al.*, 2004). In this study, we report interactions between successional development, specific functional processes (CO and hydrogen oxidation and acetylene reduction) and related microbiological and biogeochemical variables for Kilauea volcano deposits with uniform ages and climatic regimes.

Data from both PP and MU sites show that atmospheric CO uptake contributes significantly (6–10%) to total respiratory activity (measured as CO_2 production) in unvegetated areas characterized by very low respiration rates and organic carbon concentrations (Tables 1 and 2). Atmospheric CO uptake rates at PP and MU unvegetated sites are similar to previously reported estimates (King, 2003a); CO_2 production rates fall within ranges reported for other organic carbon poor systems (Hopkins *et al.*, 2007). These observations support a role for CO as an energy source in carbon-limited systems, even when it is available at only very low concentrations (75–125 p.p.b.).

In contrast, atmospheric CO contributes little or nothing to respiratory activity at PP-canopy and -edge and MU-veg sites (Table 2). Even accounting for the possibility that root respiration might contribute a significant fraction of total respiration at these sites (up to about 50%; Andrews *et al.*, 1999; Wang *et al.*, 2005), CO oxidation remains a minor fraction of bacterial activity. Instead, at these sites rhizodeposition and leaf litter no doubt represent the primary sources of organic matter for respiration. These carbon sources support respiration rates for the PP and MU at levels similar to those reported for other vegetated systems with moderate-to-high organic carbon concentrations (Campbell and Law, 2005; Vogel *et al.*, 2005; Bernhardt *et al.*, 2006).

All of the sites assayed consume atmospheric hydrogen, but there is little consistent variation among them (Table 2). Relative to carbon-based respiratory metabolism, atmospheric hydrogen uptake supports considerable activity (Table 2). At sites MU-unveg and PP-bare, where organic carbon is limited, hydrogen uptake could contribute to biosynthesis, but CO_2 fixation efficiencies are relatively low with hydrogen lithotrophy (Bowien and Schlegel, 1981), and some hydrogen uptake appears due to exoenzymatic activity (King, 2003a).

Although atmospheric CO contributes significantly to bacterial metabolism at unvegetated sites, CO-oxidizing bacteria were active at all sites. This is evident from time courses of headspace CO concentrations during both *in situ* and *ex situ* analyses (not shown). As in previous studies (King, 1999), a model for CO change based on a zero-order production term and a first-order uptake term explained patterns of CO uptake and emission. In addition, cinders from all PP and MU sites consume exogenous CO added at elevated concentrations without a lag. Maximum potential CO uptake rates based on these assays correlate linearly with estimates of microbial biomass (Figure 1b), and depth integrated maximum potential rates for PP correlate linearly with respiration rates (Figure 3). To the extent that maximum potential CO uptake rates reflect CO oxidizer biomass, these relationships indicate that CO oxidizer biomass accounts for an approximately constant fraction of total biomass, and that maximum potential activity likely responds to the same variables that determine respiratory activity.

In particular, it appears that CO oxidizer biomass may become initially established on barren deposits through inputs of atmospheric CO and exogenous organic matter (for example, in precipitation). Subsequently, CO oxidizer biomass expands with endogenous organic matter production, especially that from rooted vegetation. This is consistent with both the preference of CO-oxidizing bacteria for organic substrates, and with their expression of CO oxidation when substrate availability is low, as is typically the case in soil systems even when bulk organic concentrations are high (Morita, 1997).

The distribution of maximum potential hydrogen uptake rates among sites parallels that for maximum potential CO uptake rates (Table 2), suggesting some common controls for the two activities. This could be due in part to the fact that some CO oxidizers also oxidize hydrogen (King and Weber, 2007). In addition, many hydrogen oxidizers, like virtually all CO oxidizers, are facultative lithotrophs that grow preferentially with organic substrates (Bowien and Schlegel, 1981). However, when plotted as paired data, maximum potential hydrogen uptake rates increase exponentially to an asymptote as a function of maximum potential CO uptake rates (Figure 3). This may reflect a shift from populations that oxidize both CO and hydrogen to populations that oxidize primarily CO as maximum potential CO uptake rates increase.

The fact that CO oxidizers remain active across a gradient of increasing ecosystem development, even though atmospheric CO decreases in significance as a substrate, indicates that they may contribute to a variety of functions other than trace gas dynamics. Many CO-oxidizing isolates contain nitrogenase (King, 2003b). Some, such as CO-oxidizing rhizobia (for example, *Bradyrhizobium japonicum* USDA 6) contribute to symbiotic nitrogen fixation; others, such as CO-oxidizing *Burkholderia* (for example, *B. xenovorans* LB400), can contribute to both asymbiotic and plant-associated nitrogen fixation (Chen *et al.*, 2003; Choudhury and Kennedy, 2004).

An exponential correlation between depth-integrated maximum potential CO uptake and a surrogate measure of nitrogen fixation, acetylene reduction, for the PP sites indicates that controls of activity differ for the two processes, irrespective of the extent of contributions by CO oxidizers. Differential controls for expression of the aerobic carbon monoxide dehydrogenase and nitrogenase systems likely include nitrogen and organic matter availability, associative interactions with plant roots and responses to physical–chemical variables, for example, pH and water potential. In addition, populations of strictly heterotrophic nitrogen fixers may proliferate to a much greater extent than nitrogen-fixing CO oxidizers in material at the canopy site, where acetylene reduction rates appear disproportionately high. Of course, variations in acetylene reduction rates among sites may only partially reflect patterns in nitrogen fixation, since ratios of acetylene reduced to nitrogen fixed may also vary among sites.

Plant roots also affect the distribution and activity of CO oxidizers. Maximum potential CO uptake rates for MU and PP sites rise exponentially with root mass to an asymptote in PP-edge and PP-canopy sites (Figure 4). This trend likely reflects an increase in organic matter availability that can support CO oxidizer biomass, but may also reflect an increase in CO availability. In particular, roots of all three plant species examined in this study emit CO at rates comparable to rates previously reported for other

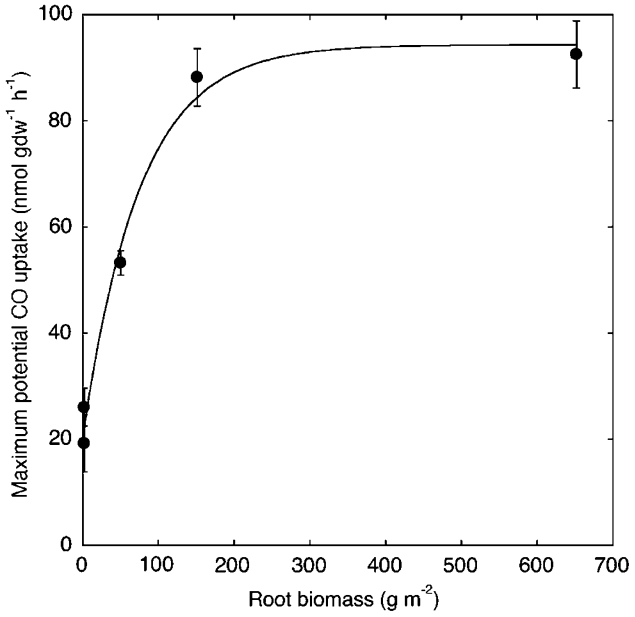

Figure 4 Maximum potential CO uptake rates integrated over 0- to 10-cm depth intervals for PP-bare, -edge and -canopy sites versus respiration rates. All data are means of triplicates ±1 s.e. Curve represents a linear least-squares best fit ($r^2 = 0.99$).

plants (Table 3; King and Crosby, 2002). As a result, increases in root biomass across sites represent a gradient of increasing CO within the deposits, which may promote CO oxidizer biomass or activity. In addition, the ability of roots of all three taxa to consume CO (Table 3) indicates that they may support CO oxidizer populations that can affect bulk and rhizosphere activities as well as exchanges with the atmosphere (King and Crosby, 2002; King and Hungria, 2002). Interactions between plants and the diversity of CO-oxidizing populations are being assessed at present.

In conclusion, atmospheric CO supports significant metabolic activity on volcanic deposits lacking vascular plant growth. Relationships between maximum potential CO uptake, root mass, organic carbon and estimates of microbial biomass indicate that subsequent to colonization on barren material, CO-oxidizing populations expand in concert with the microbial community as a whole, even though the role of CO in metabolism overall diminishes with increasing plant development. CO oxidizers remain an active component of the microbial community throughout succession and may contribute to nitrogen fixation, rates of which increase through successional development.

References

Andrews JA, Harrison KG, Matamala R, Schlesinger WH. (1999). Separation of root respiration from total soil respiration using carbon-13 labeling during free-air carbon dioxide enrichment (FACE). *Soil Sci Soc Am J* **63**: 1429–1435.

Bernhardt ES, Barber JJ, Pippen JS, Taneva L, Andrews JA, Schlesinger WH. (2006). Long-term effects of free air CO_2 enrichment (FACE) on soil respiration. *Biogeochemistry* **77**: 91–116.

Bowien B, Schlegel HG. (1981). Physiology and biochemistry of aerobic hydrogen-oxidizing bacteria. *Annu Rev Microbiol* **35**: 405–452.

Brinch-Iversen J, King GM. (1990). Effects of substrate concentration, growth state, and oxygen availability on relationships among bacterial carbon, nitrogen and phospholipid phosphorous content. *FEMS Microbiol Ecol* **74**: 345–355.

Campbell JL, Law BE. (2005). Forest soil respiration across three climatically distinct chronosequences in Oregon. *Biogeochemistry* **73**: 109–125.

Chadwick OA, Derry LA, Vitousek PM, Huebert BJ, Hedin LO. (1999). Changing sources of nutrients during four million years of ecosystem development. *Nature* **397**: 491–497.

Chen W-M, Moulin L, Bontemps C, Vandamme P, Béna G, Boivin-Masson C. (2003). Legume symbiotic nitrogen fixation by β-proteobacteria is widespread in nature. *J Bacteriol* **185**: 7266–7272.

Choudhury ATMA, Kennedy IR. (2004). Prospects and potentials for systems of biological nitrogen fixation in sustainable rice production. *Biol Fertil Soils* **39**: 219–227.

Crews TE, Kitayama K, Vitousek PM. (1995). Changes in soil phosphorus fractions and ecosystem dynamics across a long chronosequence in Hawaii. *Ecology* **76**: 1407–1424.

Crews TE, Kurina LM, Vitousek PM. (2001). Organic matter and nitrogen accumulation and nitrogen fixation during early ecosystem development in Hawaii. *Biogeochemistry* **53**: 259–279.

de Neergaard A, Gorissen A. (2004). Carbon allocation to roots, rhizodeposits and soil after pulse labeling: a comparison of white clover (*Trifolium repens* L.) and perennial ryegrass (*Lolium perenne* L.). *Biol Fertil Soils* **39**: 228–234.

Dunfield KE, King GM. (2004). Molecular analysis of carbon monoxide-oxidizing bacteria associated with recent Hawaiian volcanic deposits. *Appl Environ Microbiol* **70**: 4242–4248.

Dunfield KE, King GM. (2005). Analysis of the distribution and diversity in recent Hawaiian volcanic deposits of a putative carbon monoxide dehydrogenase large subunit gene. *Environ Microbiol* **7**: 1405–1412.

Gomez-Alvarez V, King GM, Nüsslein K. (2007). Comparative bacterial diversity in recent Hawaiian volcanic deposits of different ages. *FEMS Microbiol Ecol* **60**: 60–73.

Hooper DU, Vitousek PM. (1997). The effects of plant composition and diversity on ecosystem processes. *Science* **277**: 1302–1305.

Hopkins DW, Badalucco L, English LC, Meli SM, Chudek JA, Ioppolo A. (2007). Plant litter decomposition and microbial characteristics in volcanic soils (Mt. Etna) at different stages of development. *Biol Fertil Soils* **43**: 461–469.

Kent AD, Triplett EW. (2002). Microbial communities and their interactions in soil and rhizosphere ecosystems. *Annu Rev Microbiol* **56**: 211–236.

King GM. (1999). Attributes of atmospheric carbon monoxide oxidation in Maine forest soils. *Appl Environ Microbiol* **65**: 5257–5264.

King GM. (2003a). Contributions of atmospheric CO and hydrogen uptake to microbial dynamics on recent

Hawaiian volcanic deposits. *Appl Environ Microbiol* **69**: 4067–4075.
King GM. (2003b). Molecular and culture-based analyses of aerobic carbon monoxide oxidizer diversity. *Appl Environ Microbiol* **69**: 7257–7265.
King GM, Crosby H. (2002). Impacts of plant roots on soil CO cycling and soil–atmosphere CO exchange. *Glob Chang Biol* **8**: 1085–1093.
King GM, Hungria M. (2002). Soil–atmosphere CO exchanges and microbial biogeochemistry of CO transformations in a Brazilian agroecosystem. *Appl Environ Microbiol* **68**: 4480–4485.
King GM, Weber CF. (2007). Distribution, diversity and ecology of aerobic CO-oxidizing bacteria. *Nat Rev Microbiol* **5**: 107–118.
Kitayama K, Mueller-Dombois D, Vitousek PM. (1995). Primary succession of Hawaiian montane rain forest on a chronosequence of eight lava flows. *J Veg Sci* **6**: 211–222.
Morisada K, Imaya A, Ono K. (2002). Temporal changes in organic carbon of soils developed on volcanic andesitic deposits in Japan. *For Ecol Manage* **171**: 113–120.
Morita RY. (1997). Bioavailability of organic matter in the environment. In: Morita RY (ed). *Bacteria in Oligotrophic Environments: Starvation–Survival Lifestyle*. Chapman & Hall: New York, NY, USA, pp 69–134.
Nanba K, King GM, Dunfield K. (2004). Analysis of facultative lithotroph distribution and diversity on volcanic deposits by use of the large subunit of ribulose-1,5-bisphosphate carboxylase/oxygenase. *Appl Environ Microbiol* **70**: 2245–2253.
Neff JC, Hobbie SE, Vitousek PM. (2000). Nutrient and mineralogical control on dissolved organic C, N and P fluxes and stoichiometry in Hawaiian soils. *Biogeochemistry* **51**: 283–302.
Nüsslein K, Tiedje JM. (1998). Characterization of the dominant and rare members of a young Hawaiian soil bacterial community with small-subunit ribosomal DNA amplified from DNA fractionated on the basis of its guanine and cytosine. *Appl Environ Microbiol* **64**: 1283–1293.
Ohta H, Ogiwara K, Murakami E, Takahashi H, Sekiguchi M, Koshida K *et al.* (2003). Quinone profiling of bacterial populations developed in the surface layer of volcanic mudflow deposits from Mt. Pinatubo (The Philippines). *Soil Biol Biochem* **35**: 1155–1158.
Ohtonen R, Hannu F, Pennanen T, Jumpponen A, Trappe J. (1999). Ecosystem properties and microbial community changes in primary succession on a glacier forefront. *Oecologia* **119**: 239–246.
Ohtonen R, Väre H. (1998). Vegetation composition determines microbial activities in a boreal forest soil. *Microb Ecol* **36**: 328–335.
Pearson HL, Vitousek PM. (2001). Stand dynamics, nitrogen accumulation, and symbiotic nitrogen fixation in regenerating stands of *Acacia koa*. *Ecol Appl* **11**: 1381–1394.
Riley RH, Vitousek PM. (1995). Nutrient dynamics and nitrogen trace gas flux during ecosystem development in montane rain forest. *Ecology* **76**: 292–304.
Schippers LA, Degens BP, Sparling GP, Duncan LC. (2001). Changes in microbial heterotrophic diversity along five plant successional sequences. *Soil Biol Biochem* **33**: 2093–2103.
Sigler WV, Crivii S, Zeyer J. (2002). Bacterial succession in glacial forefield soils characterized by community structure, activity and opportunistic growth dynamics. *Microb Ecol* **44**: 306–316.
Sigler WV, Zeyer J. (2002). Microbial diversity and activity along the forefields of two receding glaciers. *Microb Ecol* **43**: 397–407.
Smolander A, Kitunen V. (2002). Soil microbial activities and characteristics of dissolved organic C and N in relation to tree species. *Soil Biol Biochem* **34**: 651–660.
Vitousek PM. (1999). Nutrient limitation to nitrogen fixation in young volcanic sites. *Ecosystems* **2**: 505–510.
Vitousek PM, Farrington H. (1997). Nutrient limitation and soil development: experimental test of a biogeochemical theory. *Biogeochemistry* **37**: 63–75.
Vogel JG, Valentine DW, Ruess RW. (2005). Soil and root respiration in mature Alaskan black spruce forests that vary in soil organic matter decomposition rates. *Can J For Res* **35**: 161–174.
Wang W, Ohse K, Liu J, Mo W, Oikawa T. (2005). Contribution of root respiration to soil respiration in a C3/C4 mixed grassland. *J Biosci* **30**: 507–514.